

# Environmentally-Sensitive Theory of Electronic and Optical Transitions in Atomically-Thin Semiconductors

Yeongsu Cho and Timothy C. Berkelbach\*

Department of Chemistry and James Franck Institute, University of Chicago, Chicago, Illinois 60637, USA

We present an electrostatic theory of band gap renormalization in atomically-thin semiconductors that captures the strong sensitivity to the surrounding dielectric environment. In particular, our theory aims to correct known band gaps, such as that of the three-dimensional bulk crystal. Combining our quasiparticle band gaps with an effective mass theory of excitons yields environmentally-sensitive optical gaps as would be observed in absorption or photoluminescence. For an isolated monolayer of MoS<sub>2</sub>, the presented theory is in good agreement with *ab initio* results based on the *GW* approximation and the Bethe-Salpeter equation. We find that changes in the electronic band gap are almost exactly offset by changes in the exciton binding energy, such that the energy of the first optical transition is nearly independent of the electrostatic environment, rationalizing experimental observations.

**Introduction.** Atomically-thin materials exhibit remarkable electronic properties due to their quasi-two-dimensional nature [1–4]. However, their size also makes them extremely sensitive to their local environment. A complete theoretical picture must simultaneously treat the two-dimensional nature of carriers and the dielectric character of the surroundings. This latter property is the primary distinction between atomically-thin materials (such as the transition metal dichalcogenides) and heterostructured semiconductor quantum wells (such as GaAs in AlGaAs).

To date, many theoretical studies of atomically-thin materials have focused on the excitonic properties, including the large exciton binding energy [5–7], the unique excitonic Rydberg series [8, 9], the nature of selection rules [10–12], and Berry phase modifications of the exciton spectrum [13, 14]. Surprisingly, the quasiparticle band gap has received significantly less attention, especially from simplified microscopic theories, perhaps because it is challenging to measure experimentally. In fact, simple theories of the exciton binding energy are often times used in conjunction with the experimentally measured optical gap in order to estimate the quasiparticle band gap [8, 15].

The *GW* approximation represents the current method-of-choice for the accurate calculation of band structures and band gaps [16, 17]. However, the quasi-two-dimensional nature of the atomically-thin materials makes these calculations very challenging to converge [18–20]. In this work, we provide a simple electrostatic theory of band gap renormalization due to electrostatic proximity effects. Through combination with an effective mass theory of the exciton binding energy, we find that the optical gap – i.e. the sum of the band gap and the (negative) exciton binding energy – is extremely insensitive to the dielectric environment. To the best of our knowledge, this represents the first quasi-analytical demonstration of this remarkable effect.

The band gap of nanoscale materials differs from that of the bulk parent material because of two separate effects: carrier confinement and dielectric contrast. In the first case, the geometric confinement of carriers leads to an increased kinetic energy and a concomitantly larger band gap. However, in layered materials (such as the TMDCs), the two-dimensional

confinement is already largely reflected in the bulk band gap, as evidenced by the small bandwidth in the perpendicular (stacking) direction. Therefore, in the following, we employ this idealized scenario of carriers confined to two dimensions, even when describing the bulk material. In particular, this approximation is invoked to describe low-energy carriers at the K-points of the Brillouin zone; here, the wavefunction character is primarily that of transition-metal *d*-orbitals, which are confined to the center of the TMDC layer, precluding strong interlayer hybridization. In Fig. 1, we show the bandstructure of bulk and monolayer MoS<sub>2</sub> calculated using density functional theory [21]. The monolayer band gap at the K-point is only 0.09 eV larger than that of the bulk, indicating that any band gap renormalization due to carrier confinement is already (largely) accounted for in the bulk band gap; we henceforth neglect this small shift so as to focus on alternative effects while treating the monolayer and bulk on equal footing. We emphasize that this geometric carrier confinement is a one-electron (kinetic energy) effect that is well-described by density functional theory – unlike dielectric screening effects.

As mentioned above, a second source of band gap renormalization in nanomaterials is the dielectric contrast effect. Physically, we recall that the quasiparticle conduction and valence bands measure the electron affinities and ionization potentials, respectively. The excess charge created in these pro-

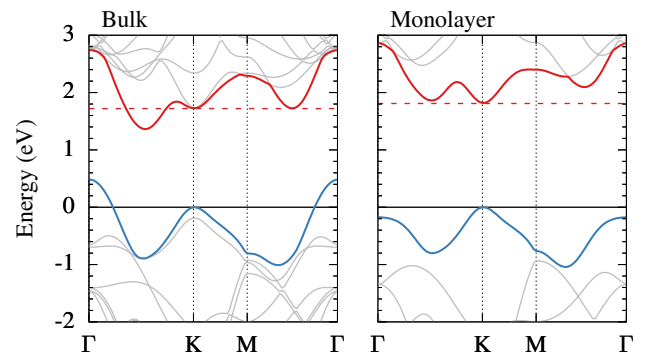


FIG. 1. Band structure of bulk and monolayer MoS<sub>2</sub> calculated with density functional theory. The direct band gap (at the K-point) is 0.09 eV larger for the monolayer than for the bulk, due to the carrier confinement effect.

cesses polarizes the material and its environment such that the potential energy of the charge depends on the local dielectric geometry. We model atomically-thin semiconductors as a slab of dielectric constant  $\varepsilon_1$  and width  $d$ , surrounded by environmental dielectric constants  $\varepsilon_2$  below and  $\varepsilon_3$  above, as shown in Fig. 2. Consistent with the arguments presented above, the carriers will be assumed to occupy the center of the slab, at  $z = 0$ .

We now proceed to calculate the band structure corrections due to such a heterogeneous dielectric environment. We assume that a *reference* many-body band gap is known, which could come from experiment or calculation. In particular, we will primarily consider band structure corrections to the three-dimensional bulk material. Corrections will be calculated in two ways: (1) classically, using electrostatic continuum theory; and (2) quantum mechanically, using the static Coulomb-hole plus screened exchange (COHSEX) approximation to the quantum mechanical  $GW$  self-energy. When correcting a reference band structure, we require the *difference* in the screened Coulomb interaction,  $\delta W(\mathbf{r}, \mathbf{r}') \equiv W(\mathbf{r}, \mathbf{r}') - W^{\text{ref}}(\mathbf{r}, \mathbf{r}')$ , where  $W$  is the total screened Coulomb interaction. We calculate the respective screened interactions through their electrostatic counterparts associated with the slab dielectric geometry shown in Fig. 2. While this is a classical approximation, which neglects local field effects, it avoids the high cost of an ab initio calculation of the screened Coulomb interaction.

In recent years, effective mass theories of atomically-thin materials have made frequent use of the model potential energy derived by Rytova [22] and Keldysh [23] (RK),

$$W^{\text{RK}}(\rho) = \frac{\pi e^2}{(\varepsilon_2 + \varepsilon_3)\rho_0} \left[ H_0\left(\frac{\rho}{\rho_0}\right) - Y_0\left(\frac{\rho}{\rho_0}\right) \right] \quad (1)$$

where  $H_0$  and  $Y_0$  are the Struve function and the Bessel function of the second kind and  $\rho$  is the two-dimensional in-plane separation. The screening length is given by  $\rho_0 = \varepsilon_1 d / (\varepsilon_2 + \varepsilon_3)$  and can be related to a two-dimensional sheet polarizability [5, 24]. For the purposes of the present manuscript, the RK potential suffers from two deficiencies. First, it applies only in the limit of extreme dielectric mismatch between the slab and its surroundings; while this approximation is good for isolated (suspended) monolayers, it breaks down in more general dielectric environments. Second, the RK potential has an unphysical logarithmic divergence at  $\rho = 0$ , which precludes its use in simple electrostatic theories of band gap renormalization. Instead, we employ the exact solution of the finite-thickness electrostatic problem shown in Fig. 2. We emphasize that the logarithmic behavior of the RK potential is correct over some intermediate length scale and only incorrect for  $\rho \lesssim d$ .

The potential energy of two charges in a slab with locations  $z_1, z_2$ , and in-plane separation  $\rho$  can be calculated via image charges to give a screened interaction  $W(z_1, z_2, \rho)$  [25]. In the

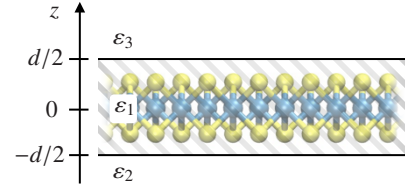


FIG. 2. Idealized dielectric slab geometry used to model the electrostatics of atomically-thin semiconductors.

center of the slab ( $z_1 = z_2 = 0$ ), we find

$$W(\rho) = \frac{e^2}{\varepsilon_1 \rho} + 2 \sum_{n=1}^{\infty} \frac{e^2 L_{12}^n L_{13}^n}{\varepsilon_1 \{\rho^2 + (2nd)^2\}^{1/2}} + (L_{12} + L_{13}) \sum_{n=0}^{\infty} \frac{e^2 L_{12}^n L_{13}^n}{\varepsilon_1 \{\rho^2 + [(2n+1)d]^2\}^{1/2}} \quad (2)$$

where  $L_{1n} = (\varepsilon_1 - \varepsilon_n) / (\varepsilon_1 + \varepsilon_n)$ . Unlike the RK potential, this continuum electrostatic potential is correct in the uniform case  $\varepsilon_1 = \varepsilon_2 = \varepsilon_3$  and has the proper divergence as  $\rho \rightarrow 0$ .

*Electrostatic solution.* In the simplest electrostatic (Born) approximation, the conduction and valence band corrections in the center of the slab are given by the self-interaction energy [25, 26]

$$\delta \Sigma_{c/v} = \pm \frac{1}{2} \lim_{\rho \rightarrow 0} \delta W(\rho), \quad (3)$$

which is non-divergent due to the use of an interaction difference,  $\delta W$ , as long as the slab dielectric  $\varepsilon_1$  is identical in both  $W$  and  $W^{\text{ref}}$ . When the reference potential energy is that of a uniform, bulk dielectric, i.e.  $W^{\text{ref}}(\mathbf{r}, \mathbf{r}') = e^2 / (\varepsilon_1 |\mathbf{r} - \mathbf{r}'|)$ , then the electrostatic corrections using Eqs. (2) and (3) can be summed analytically to give the relatively simple expression

$$\delta \Sigma_{c/v} = \pm \frac{e^2}{2\varepsilon_1 d} \left\{ \frac{2(L_{12} + L_{13})}{\sqrt{L_{12}L_{13}}} \tanh^{-1} \left( \sqrt{L_{12}L_{13}} \right) - \log(1 - L_{12}L_{13}) \right\}. \quad (4)$$

*Tight-binding COHSEX.* First-principles band structure calculations typically employ the  $GW$  approximation to the self-energy. In the static screening limit, this approximation yields two contributions to the self-energy: a Coulomb-hole (COH) term and a screened exchange (SEX) term [16]. By assuming that an initial, many-body *reference* band structure is known, we can calculate corrections in alternative electrostatic environments as diagonal elements of the self-energy operator, which leads to

$$\delta \Sigma_p^{\text{COH}}(\mathbf{k}) = \frac{1}{2} \lim_{\rho \rightarrow 0} \delta W(\rho), \quad (5a)$$

$$\delta \Sigma_p^{\text{SEX}}(\mathbf{k}) = -\frac{1}{N_k} \int d^2 x_1 \int d^2 x_2 \phi_{p,\mathbf{k}}^*(x_1) \rho(x_1, x_2) \times \delta W(\rho) \phi_{p,\mathbf{k}}(x_2), \quad (5b)$$

where  $\mathbf{x} = (\rho, \tau)$  is the combined space and spin variable,  $\rho(\mathbf{x}_1, \mathbf{x}_2)$  is the reduced density matrix of the mean-field reference,  $N_k$  is the number of  $k$ -points sampled in the Brillouin zone, and  $p = (c, v)$  indexes the conduction or valence band. In the simplest approximation, we consider the two-band tight-binding Hamiltonian [27]

$$H(\mathbf{k}) = \begin{pmatrix} E_g/2 & at(k_x + ik_y) \\ at(k_x - ik_y) & -E_g/2 \end{pmatrix} \quad (6)$$

with eigenvectors  $\langle \mathbf{x} | p\mathbf{k} \rangle = \phi_{p\mathbf{k}}(\mathbf{x})$  and eigenvalues  $E_{c/v}(\mathbf{k}) = \pm \frac{1}{2} \sqrt{E_g^2 + (2atk)^2}$ . In this Hamiltonian,  $E_g$  is the band gap,  $a$  is the lattice constant, and  $t$  is the interatomic transfer integral. A single (doubly-occupied) valence band leads to the simple density matrix  $\rho(\mathbf{x}_1, \mathbf{x}_2) = \sum_{\mathbf{q}} \phi_{v\mathbf{q}}(\mathbf{x}_1) \phi_{v\mathbf{q}}^*(\mathbf{x}_2)$ . Further simplifications concerning the locality of the underlying real-space basis functions leads to the SEX self-energy

$$\delta\Sigma_p^{\text{SEX}}(\mathbf{k}) = -\frac{1}{N_k} \sum_{\mathbf{q}} |\langle v\mathbf{k} | v\mathbf{q} \rangle|^2 \sum_{\mathbf{G}}' \delta W(\mathbf{G} + \mathbf{q} - \mathbf{k}), \quad (7)$$

where

$$\delta W(\mathbf{k}) = \frac{1}{A_{\text{BZ}}} \int d^2\rho e^{i\rho \cdot \mathbf{k}} \delta W(\rho), \quad (8)$$

$A_{\text{BZ}}$  is the area of the Brillouin zone, and the primed summation in Eq. (7) excludes the term with  $\mathbf{G} = 0$  when  $\mathbf{k} = \mathbf{q}$ . Summarizing, the COH term yields a positive, constant shift to both the conduction and valence band, which is *exactly* equal to the (positive) correction obtained in the pure electrostatic theory presented above; the SEX term yields a negative,  $k$ -dependent shift with a magnitude that depends on overlap factors between the valence band and the band being corrected. To a reasonable approximation (verified numerically below), the SEX contribution is negligible in the conduction band (due to vanishing overlaps) but is substantial in the valence band. Further, if the squared overlap is approximated by unity, i.e.  $|\langle v\mathbf{k} | v\mathbf{q} \rangle|^2 \approx 1$ , then the magnitude of the SEX correction in the valence band is exactly twice that of the COH term. As shown in Ref. 28 for the case of molecules near metal surfaces, we therefore have simple, approximate COHSEX corrections given by  $\delta\Sigma_c \approx +P - 0 = +P$  and  $\delta\Sigma_v \approx +P - 2P = -P$ , where  $P = \frac{1}{2} \lim_{\rho \rightarrow 0} \delta W(\rho)$  is precisely the electrostatically-derived correction. In reality, the squared overlap can be less than one, and the SEX correction to the valence band (and thus the band gap) will be slightly smaller than that of the continuum electrostatic theory.

*Effective-mass theory of excitons.* The optical gap, as measured in linear spectroscopies such as absorption or photoluminescence, is the sum of the quasiparticle band gap and the (negative) exciton binding energy. At a similar level of theory to that used so far, the exciton states can be calculated using an effective mass theory,

$$\left[ -\frac{1}{2\mu} \nabla_{\rho}^2 - W(\rho) \right] \Psi_n(\rho) = E_n \Psi_n(\rho), \quad (9)$$

where  $\rho$  is the electron-hole separation,  $\Psi_n$  is the exciton wavefunction, and  $E_n$  is its binding energy. The material parameters enter through the exciton reduced mass  $\mu = m_e m_h / (m_e + m_h)$  and the same screened Coulomb interaction  $W$  as used above. Due to the angular symmetry, the effective mass equation is a simple one-dimensional Schrödinger equation in the radial direction, which may be solved numerically exactly on a real-space grid to obtain the full Rydberg series of band-edge excitons. The exciton wavefunctions and binding energies are sensitive to the local dielectric environment, where higher dielectric constants result in stronger screening, more diffuse wavefunctions, and smaller binding energies.

*Results.* While our theory is appropriate for any atomically-thin semiconductor, we will apply it to the well-studied case of MoS<sub>2</sub>, a prototypical layered transition-metal dichalcogenide. As is common for quantum-confined materials, we correct the bulk band gap using a uniform reference Coulomb potential with  $\epsilon_1 = \epsilon_2 = \epsilon_3$ , i.e.  $W^{\text{ref}}(\mathbf{r}, \mathbf{r}') = e^2 / (\epsilon_1 |\mathbf{r} - \mathbf{r}'|)$  [29]; for MoS<sub>2</sub>, we use  $\epsilon_1 = 14$ . For the monolayer, we solve the electrostatic problem in Fig. 2 with  $\epsilon_1 = 14$  and  $d = 6 \text{ \AA}$ , which roughly corresponds to the perpendicular extent of monolayer MoS<sub>2</sub>; these parameters yield the ideal screening length  $\rho_0 = 42 \text{ \AA}$  in good agreement with the ab initio value of  $41.5 \text{ \AA}$  [5]. We take the reference A-series band gap of bulk MoS<sub>2</sub> to be  $E_g^{\text{bulk}} = 1.98 \text{ eV}$  [30] and for the tight-binding Hamiltonian in Eq. (6), we use  $at = 3.51 \text{ eV} \cdot \text{\AA}$ .

First, we consider the experimentally-relevant situation of a monolayer on a substrate with dielectric constant  $\epsilon_2$  and vacuum above ( $\epsilon_3 = 1$ ). In Fig. 3(a), we show the band gap calculated using the tight-binding COHSEX approximation, as a function of the substrate dielectric constant. The purely electrostatic approximation in Eq. (4) is not shown, but gives nearly identical results, predicting band gaps that are slightly larger (about 0.05 eV), which can be understood based on arguments presented above. Remarkably, the simple theory pre-

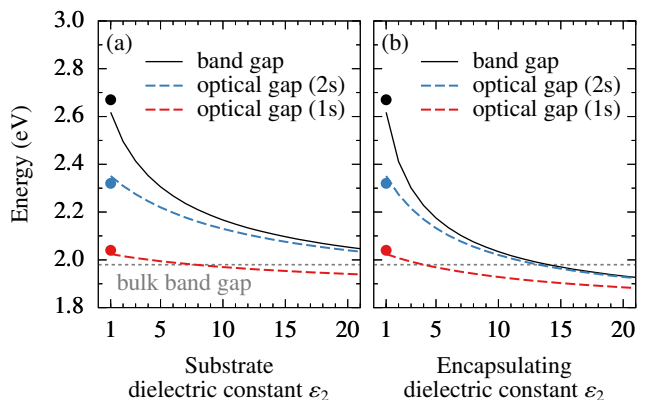


FIG. 3. Quasiparticle band gap and optical gap (i.e. excitonic transition energy) as a function of (a) the substrate dielectric constant with vacuum above ( $\epsilon_3 = 1$ ), and (b) the encapsulating dielectric constant ( $\epsilon_2 = \epsilon_3$ ). The bulk band gap, which is a fixed parameter in the theory, is indicated by a dotted grey line. Filled circles at  $\epsilon_2 = 1$  indicate the ab initio  $G_0W_0$  result (black circle) and the Bethe-Salpeter equation results (red and blue circles) for an isolated monolayer, from Ref. 20.

sented here – parameterized only on bulk data and an estimate of the monolayer width – predicts an isolated monolayer ( $\epsilon_2 = 1$ ) band gap of 2.62 eV (a 0.64 eV increase from bulk); this compares very favorably to a recent, carefully-converged ab initio calculation using the many-body  $G_0W_0$  approximation, which predicts 2.67 eV [20]. This huge increase in the quasiparticle band gap reflects the strong role played by reduced dielectric screening in atomically-thin materials.

At larger values of  $\epsilon_2$ , the increased screening ability of the substrate yields a rapid decrease in the band gap, demonstrating the strong sensitivity of atomically-thin materials to their local environment. Even a modest substrate like silica, with a dielectric constant of  $\epsilon_2 \approx 4$ , is predicted to have a band gap of 2.35 eV, which is 0.27 eV smaller than an ideal, suspended monolayer. On graphite, with  $\epsilon_2 \approx 10$ , the band gap is reduced by 0.45 eV. Similar results have been obtained with an approximate treatment of substrate screening in otherwise ab initio  $G_0W_0$  calculations [31, 32]. These findings underscore the care required when comparing experimental measurements on substrates to ab initio calculations of isolated atomically-thin materials. In reverse, the simple formula given in Eq. (4) can be used to infer the ideal, suspended band gap based on measurements performed on substrates.

In Fig. 3(a), we also show the optical gap for the 1s and 2s exciton states, obtained by summing the quasiparticle band gap and the exciton binding energies of each state, as a function of the substrate dielectric constant. For the isolated monolayer, we predict optical gaps of 2.03 eV and 2.35 eV (positive binding energies of 0.59 eV and 0.27 eV) for the 1s and 2s states, respectively. Again, these compare well with converged ab initio calculations using the Bethe-Salpeter equation, which predict optical gaps of 2.04 eV and 2.32 eV (binding energies of 0.63 eV and 0.35 eV) [20].

As the dielectric constant of the substrate increases, the exciton binding energies are reduced due to increased environmental screening. Remarkably, the competing effects in the band gap and 1s binding energy almost exactly cancel. Up to a substrate dielectric constant of  $\epsilon_2 = 20$ , the 1s optical transition energy only changes by 0.1 eV. In the aforementioned examples of silica and graphite substrates, the exciton binding energy is reduced by 0.24 eV and 0.49 eV, respectively. Not only is the optical transition energy roughly constant, but the cancellation is almost perfect such that the monolayer transition energy is nearly identical to the bulk transition energy (the bulk band gap and optical gap roughly coincide, because the exciton binding energy is only about 0.04 eV [30]).

In addition to the well-known observation that the optical gap of bulk TMDCs is almost identical to that of monolayers, the effects predicted by the theory are in good agreement with a number of other more detailed experimental findings, such as the insensitivity of the optical gap in TMDCs when comparing suspended samples and samples on fused silica substrates [33]. Identical effects in the band gap, optical gap, and exciton binding energy have been observed in a joint experimental-computational study of  $\text{MoSe}_2$  on bilayer graphene and graphite: the latter exhibits a 0.24 eV reduction

in the band gap and a concomitant 0.28 eV reduction in the exciton binding energy, leading to a minimal change in the optical gap [31].

The above analysis can be repeated for more general dielectric environments; the results of uniform encapsulation ( $\epsilon_2 = \epsilon_3$ ) are shown in Fig. 3(b). While the qualitative behavior is the same, the effects are naturally stronger due to the simultaneous screening from above and below the monolayer.

Finally, we mention that although we have focused on the band gap, our theory separately predicts changes to the ionization potential and electron affinity. The environmental renormalization of these quantities may be of interest for photochemistry, catalysis, or device engineering.

*Conclusions.* In summary, we have presented a simple, but powerful theory of environmentally-sensitive electronic and optical transition energies in atomically-thin materials. While the theory shows that the quasiparticle band gap and the exciton binding energy are individually very sensitive to their local dielectric environment, the sum of the two (the lowest-energy optical transition) is almost completely insensitive. In some sense, this is an unfortunate state of affairs for the use of atomically-thin materials as environmental or chemical sensors, because optical transitions are the simplest to measure (by absorption or photoluminescence); by contrast, measuring the band gap by photoemission or electron tunneling experiments is much more difficult. Nonetheless, the theory presented here enables rapid and quantitative exploration of accessible energetic changes through dielectric engineering.

In light of our results, we propose that the higher-lying excitonic resonances are promising optical reporters of the local environment. Even the 2s resonance – which can typically be resolved in experiments – is predicted to redshift by 0.1 eV when a suspended sample is placed on a silica substrate. Indeed, the 1s-2s separation was used recently as an experimental probe of environmental effects [15].

Going forward, this approach can be used to study other environmentally-sensitive, atomically-thin materials such as black phosphorous [34]. These techniques can also be applied to more heterogeneous dielectric environments, as might be experimentally realized through patterning [15], molecular coverage [35, 36], or functional layered heterostructures [37–39]. In many cases, explicit electronic hybridization and charge transfer should be accounted for in the theory. Work along these lines is currently in progress.

This work was primarily supported by the University of Chicago Materials Research Science and Engineering Center, which is funded by the National Science Foundation under Award Number DMR-1420709.

---

\* [berkelbach@uchicago.edu](mailto:berkelbach@uchicago.edu)

[1] K. F. Mak, M. Y. Sfeir, Y. Wu, C. H. Lui, J. A. Misewich, and T. F. Heinz, *Phys. Rev. Lett.* **101**, 2 (2008).

- [2] A. H. Castro Neto, F. Guinea, N. M. R. Peres, K. S. Novoselov, and A. K. Geim, *Rev. Mod. Phys.* **81**, 109 (2009).
- [3] A. Splendiani, L. Sun, Y. Zhang, T. Li, J. Kim, C.-Y. Chim, G. Galli, and F. Wang, *Nano Lett.* **10**, 1271 (2010).
- [4] K. Mak, C. Lee, J. Hone, J. Shan, and T. Heinz, *Phys. Rev. Lett.* **105**, 136805 (2010).
- [5] T. C. Berkelbach, M. S. Hybertsen, and D. R. Reichman, *Phys. Rev. B* **88**, 045318 (2013).
- [6] G. Berghäuser and E. Malic, *Phys. Rev. B* **89**, 125309 (2014).
- [7] T. Olsen, S. Latini, F. Rasmussen, and K. S. Thygesen, *Phys. Rev. Lett.* **116**, 1 (2016).
- [8] A. Chernikov, T. C. Berkelbach, H. M. Hill, A. Rigosi, Y. Li, O. B. Aslan, D. R. Reichman, M. S. Hybertsen, and T. F. Heinz, *Phys. Rev. Lett.* **113**, 076802 (2014).
- [9] D. Y. Qiu, F. H. da Jornada, and S. G. Louie, *Phys. Rev. Lett.* **111**, 216805 (2013).
- [10] T. C. Berkelbach, M. S. Hybertsen, and D. R. Reichman, *Phys. Rev. B* **92**, 085413 (2015).
- [11] P. Gong, H. Yu, Y. Wang, and W. Yao, *Phys. Rev. B* **95**, 125420 (2017).
- [12] T. Cao, M. Wu, and S. G. Louie, [arXiv:1708.02227](https://arxiv.org/abs/1708.02227).
- [13] A. Srivastava and A. Imamoglu, *Phys. Rev. Lett.* **115**, 166802 (2015).
- [14] J. Zhou, W.-Y. Shan, W. Yao, and D. Xiao, *Phys. Rev. Lett.* **115**, 166803 (2015).
- [15] A. Raja, A. Chaves, J. Yu, G. Arefe, H. M. Hill, A. F. Rigosi, T. Korn, C. Nuckolls, J. Hone, T. C. Berkelbach, P. Nagler, C. Schu, L. E. Brus, T. F. Heinz, D. R. Reichman, and A. Chernikov, *Nat. Commun.* **8**, 1521 (2017).
- [16] L. Hedin, *Phys. Rev.* **139**, 796 (1965).
- [17] M. S. Hybertsen and S. G. Louie, *Phys. Rev. Lett.* **55**, 1418 (1985).
- [18] H.-P. Komsa and A. V. Krasheninnikov, *Phys. Rev. B* **86**, 241201 (2012).
- [19] F. Hüser, T. Olsen, and K. S. Thygesen, *Phys. Rev. B* **88**, 245309 (2013).
- [20] D. Y. Qiu, F. H. da Jornada, and S. G. Louie, *Phys. Rev. B* **93**, 235435 (2016).
- [21] Density functional theory calculations were performed with the Quantum ESPRESSO software package [40], with the PBE exchange-correlation functional [41], norm-conserving pseudopotentials, and a  $12 \times 12 \times 1$  ( $12 \times 12 \times 3$ ) sampling of the Brillouin zone for the monolayer (bulk).
- [22] N. S. Rytova, *Vestn. Mosk. Univ. Fiz. Astron.* **3**, 30 (1967).
- [23] L. Keldysh, *JETP Lett.* **29**, 658 (1979).
- [24] P. Cudazzo, I. V. Tokatly, and A. Rubio, *Phys. Rev. B* **84**, 085406 (2011).
- [25] M. Kumagai and T. Takagahara, *Phys. Rev. B* **40**, 12359 (1989).
- [26] L. E. Brus, *J. Chem. Phys.* **79**, 5566 (1983).
- [27] D. Xiao, G.-B. Liu, W. Feng, X. Xu, and W. Yao, *Phys. Rev. Lett.* **108**, 196802 (2012).
- [28] J. B. Neaton, M. S. Hybertsen, and S. G. Louie, *Phys. Rev. Lett.* **97**, 1 (2006).
- [29] In reality, the screening of bulk TMDCs is anisotropic, and one could imagine using a more complicated, but realistic reference potential; however, using a coarse-grained treatment of the anisotropy,  $W^{\text{ref}}(\mathbf{r}, \mathbf{r}') = e^2 / [\epsilon_z \epsilon_{xy} \rho^2 + \epsilon_{xy}^2 (z - z')^2]^{1/2}$ , gives the same result in the order  $z \rightarrow z'$  with  $\rho = 0$ .
- [30] B. Evans and P. Young, *Proc. R. Soc. A Math. Phys. Sci.* **284**, 402 (1965).
- [31] M. Ugeda, A. Bradley, S. Shi, and H. Felipe, *Nat. Mater.* **1** (2014).
- [32] J. Ryou, Y.-S. Kim, S. KC, and K. Cho, *Sci. Rep.* **6**, 29184 (2016).
- [33] Y. Li, A. Chernikov, X. Zhang, A. Rigosi, H. M. Hill, A. M. van der Zande, D. a. Chenet, E.-M. Shih, J. Hone, and T. F. Heinz, *Phys. Rev. B* **90**, 1 (2014).
- [34] D. Y. Qiu, F. H. Da Jornada, and S. G. Louie, *Nano Lett.* **17**, 4706 (2017).
- [35] N. Peimyoo, W. Yang, J. Shang, X. Shen, Y. Wang, and T. Yu, *ACS Nano* **11**, 11320 (2014).
- [36] M. Feierabend, G. Berghäuser, A. Knorr, and E. Malic, *Nat. Commun.* **8**, 14776 (2017).
- [37] K. S. Novoselov, A. Mischenko, A. Carvalho, and A. H. Castro Neto, *Science* **353**, aac9439 (2016).
- [38] Z. Lin, A. McCreary, N. Briggs, S. Subramanian, K. Zhang, Y. Sun, X. Li, N. J. Borys, H. Yuan, S. K. Fullerton-Shirley, A. Chernikov, H. Zhao, S. McDonnell, A. M. Lindenberg, K. Xiao, B. J. LeRoy, M. Drndic, J. C. M. Hwang, J. Park, M. Chhowalla, R. E. Schaak, A. Javey, M. C. Hersam, J. Robinson, and M. Terrones, *2D Mater.* **3**, 042001 (2016).
- [39] N. R. Wilson, P. V. Nguyen, K. Seyler, P. Rivera, A. J. Marsden, Z. P. Laker, G. C. Constantinescu, V. Kandyba, A. Barinov, N. D. Hine, X. Xu, and D. H. Cobden, *Sci. Adv.* **3**, e1601832 (2017).
- [40] P. Giannozzi, S. Baroni, N. Bonini, M. Calandra, R. Car, C. Cavazzoni, D. Ceresoli, G. L. Chiarotti, M. Cococcioni, I. Dabo, A. D. Corso, S. Fabris, G. Fratesi, S. de Gironcoli, R. Gebauer, U. Gerstmann, C. Gougoussis, A. Kokalj, M. Lazzeri, L. Martin-Samos, N. Marzari, F. Mauri, R. Mazzarello, S. Paolini, A. Pasquarello, L. Paulatto, C. Sbraccia, S. Scandolo, G. Sclauzero, A. P. Seitsonen, A. Smogunov, P. Umari, and R. M. Wentzcovitch, *J. Phys. Condens. Matter* **21**, 395502 (2009).
- [41] J. P. Perdew, K. Burke, and M. Ernzerhof, *Phys. Rev. Lett.* **77**, 3865 (1996).